Journal of Magnetic Resonance 308 (2019) 106589

Contents lists available at ScienceDirect

Journal of Magnetic Resonance

journal homepage: www.elsevier.com/locate/jmr

Direct evidence for (G)O6···H_2-N4(C)$^+$ hydrogen bonding in transient G(*syn*)-C$^+$ and G(*syn*)-m^{5}C$^+$ Hoogsteen base pairs in duplex DNA from cytosine amino nitrogen off-resonance $R_{1\rho}$ relaxation dispersion measurements

Atul Rangadurai [a], Johannes Kremser [b], Honglue Shi [c], Christoph Kreutz [b,*], Hashim M. Al-Hashimi [a,c,*]

[a] Department of Biochemistry, Duke University School of Medicine, Durham, NC 27710, USA
[b] Institute of Organic Chemistry and Center for Molecular Biosciences, University of Innsbruck, Innsbruck, Austria
[c] Department of Chemistry, Duke University, Durham, NC 27710, USA

ARTICLE INFO

Article history:
Received 20 June 2019
Revised 30 August 2019
Accepted 2 September 2019
Available online 5 September 2019

This paper is dedicated to Prof. James H. Prestegard on the occasion of his 75th birthday.

Keywords:
Nucleic acid dynamics
Chemical exchange
5-Methyl cytosine
Epigenetics

ABSTRACT

NMR relaxation dispersion studies have shown that Watson-Crick G-C and A-T base pairs in duplex DNA exist in dynamic equilibrium with their Hoogsteen counterparts. Hoogsteen base pairs form through concurrent rotation of the purine base about the glycosidic bond from an *anti* to a *syn* conformation and constriction of the C1′-C1′ distance across the base pair by ~2 Å to allow Hoogsteen type hydrogen bonding. Owing to their unique structure, Hoogsteen base pairs can play important roles in DNA recognition, the accommodation, recognition, and repair of DNA damage, and in DNA replication. NMR relaxation dispersion experiments targeting imino nitrogen and protonated base and sugar carbons have provided insights into many structural features of transient Hoogsteen base pairs, including one of two predicted hydrogen bonds involving (G)N7···H-N3(C)$^+$ and (A)N7···H-N3(T). Here, through measurement of cytosine amino (N4) $R_{1\rho}$ relaxation dispersion, we provide direct evidence for the second (G)O6···H_2-N4(C)$^+$ hydrogen bond in G(*syn*)-C$^+$ transient Hoogsteen base pairs. The utility of cytosine N4 $R_{1\rho}$ relaxation dispersion as a new sensitive probe of transient Hoogsteen base pairs, and cytosine dynamics in general, is further demonstrated by measuring G(*syn*)-C$^+$ Hoogsteen exchange near neutral pH and in the context of the naturally occurring DNA modification 5-methyl cytosine (m^{5}C), in DNA samples prepared using chemical synthesis and a ^{15}N labeled m^{5}C phosphoramidite.

1. Introduction

NMR experiments employing $R_{1\rho}$ relaxation dispersion (RD) [1–4] have revealed that in duplex DNA, G-C and A-T Watson-Crick base pairs (bps) transiently adopt sparsely populated (~0.1%–1%) Hoogsteen bps [5,6]. Hoogsteen bps form through 180° rotation of the purine base about the glycosidic bond from an *anti* to a *syn* conformation [7,8] (Fig. 1A). Owing to their unique structure, Hoogsteen bps can play unique roles in DNA recognition by proteins [9,10] and antibiotics [11,12], in damage induction, accommodation [5,13–15] and repair [16,17], and in bypass of damaged bases during DNA replication [18,19] (reviewed in [20,21]). A deep understanding of the inherent propensity of DNA duplexes to form Hoogsteen bps is important to decipher the occurrence and functional roles of these non-canonical bps in DNA biochemistry.

Transient Hoogsteen bps are proposed to be stabilized by two hydrogen bonds, the formation of which requires shortening of the C1′-C1′ distance across the bp through changes in the sugar and backbone conformation, which also leads to kinking of the DNA double helix [8,15,22]. ^{15}N $R_{1\rho}$ measurements targeting the imino nitrogen atoms guanine-N1 and thymine-N3, combined with deazapurine substitution experiments have provided direct evidence for the (G)N7···H-N3(C)$^+$ and A(N7)···H-N3(T) hydrogen bonds in G(*syn*)-C$^+$ and A(*syn*)-T transient Hoogsteen bps respectively [23]. The second hydrogen bond (G)O6···H_2-N4(C)$^+$ and (A)N6-H_2···O4(T) in G(*syn*)-C$^+$ and A(*syn*)-T transient Hoogsteen bps respectively, involves the amino groups of cytosine and adenine. Interestingly, these hydrogen bonds also form in Watson-Crick bps and therefore represent an interaction that is preserved during the Watson-Crick to Hoogsteen transition. While this hydrogen bond is observed in DNA duplexes containing N^1-methylated

* Corresponding authors at: Department of Biochemistry, Duke University School of Medicine, Durham, NC 27710, USA (H.M. Al-Hashimi).
E-mail addresses: christoph.kreutz@uibk.ac.at (C. Kreutz), hashim.al.hashimi@duke.edu (H.M. Al-Hashimi).

https://doi.org/10.1016/j.jmr.2019.106589
1090-7807/

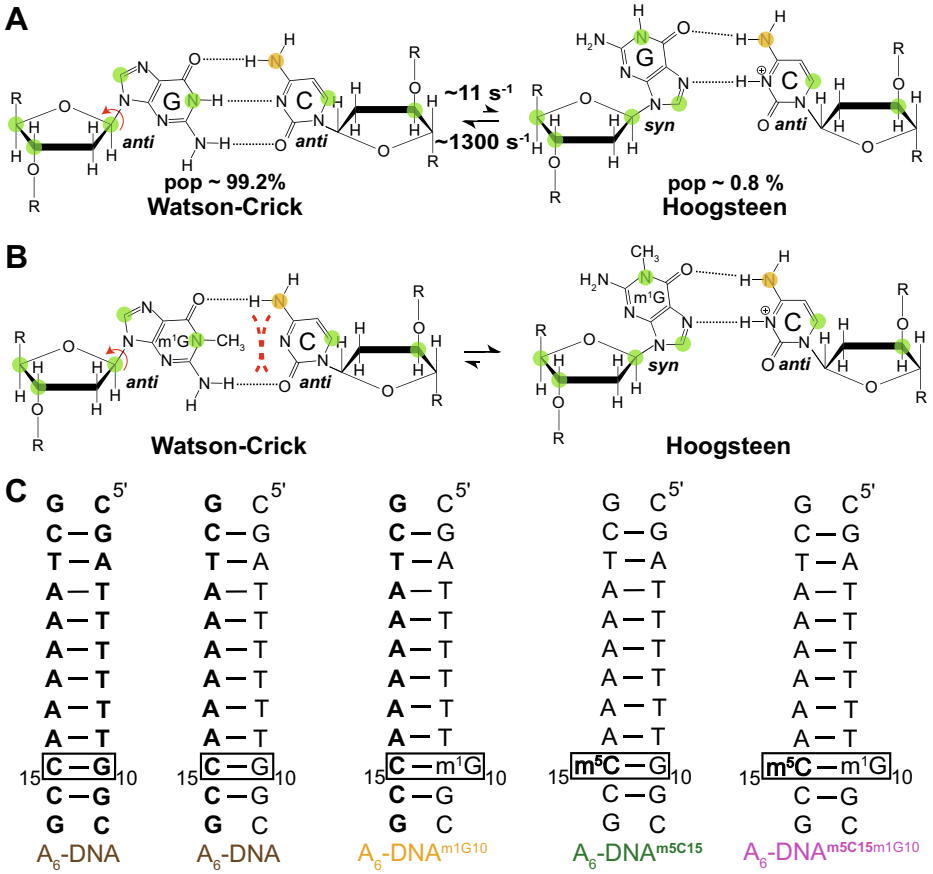

Fig. 1. Watson-Crick to Hoogsteen exchange and the DNA duplexes used in this study. (A) Watson-Crick G(*anti*)-C(*anti*) bps in B-DNA exist in dynamic equilibrium with G(*syn*)-C^+(*anti*) Hoogsteen bps, that are formed by rotation of the guanine base about the glycosidic bond (red arrow) into a *syn* conformation. Filled green circles denote nuclei that have been used to probe the Watson-Crick to Hoogsteen exchange via $R_{1\rho}$ RD measurements, while the yellow circle denotes the cytosine amino nitrogen probe used in this study. Rates and populations were obtained from RD measurements reported previously [6]. (B) m^1G destabilizes G-C Watson-Crick bps sterically (red dashes) and via the loss of a hydrogen bond acceptor, biasing the bp conformation towards Hoogsteen. (C) DNA duplexes used in this study with ^{13}C, ^{15}N labeled (A, C, T and G) or ^{15}N only labeled (m^5C) nucleotides denoted in bold. All other nucleotides are unlabeled. Black box denotes site at which formation of Hoogsteen bps was examined using NMR. (For interpretation of the references to color in this figure legend, the reader is referred to the web version of this article.)

adenine (m^1A) and guanine (m^1G) which stabilize m^1A(*syn*)-T and m^1G(*syn*)-C^+ Hoogsteen bps (Fig. 1B) [5,13,15], there is as of yet no direct evidence that this hydrogen bond also forms in unmodified transient Hoogsteen bps. The methyl group could in principle alter base stacking and favor the formation of this hydrogen bond.

Recently we demonstrated the utility of guanine amino (N2) $R_{1\rho}$ RD measurements [24] in characterizing (G)N2-H_2···O2(T) hydrogen bonds in Watson-Crick like G-T mismatches formed by tautomerization and ionization of the bases [25,26]. Here, through the measurement of cytosine amino (N4) $R_{1\rho}$ RD, we provide direct evidence for the second (G)O6···H_2-N4(C)$^+$ hydrogen bond in transient G(*syn*)-C^+ Hoogsteen bps. The utility of cytosine N4 $R_{1\rho}$ RD as a new sensitive probe of transient Hoogsteen bps, and cytosine dynamics in general, is further demonstrated by measuring G(*syn*)-C^+ Hoogsteen exchange near neutral pH and measuring Watson-Crick to Hoogsteen exchange in the context of the naturally occurring DNA modification 5-methyl cytosine (m^5C), in DNA samples prepared using chemical synthesis and a ^{15}N labeled m^5C phosphoramidite.

2. Materials and methods

2.1. Sample preparation

Unmodified and m^1G containing DNA oligonucleotides: All unmodified DNA oligonucleotides were purchased from Integrated DNA Technologies with standard desalting purification, while the A_6-DNA^{m1G10} single strand was purchased from Midland DNA technologies with cartridge purification.

Synthesis of ^{15}N isotopically labeled m^5C phosphoramidite: Two variants of the $^{15}N_3$-m^5C amidite were synthesized in the course of this project. First, a N^4-acetyl (N^4-Ac) protected variant was synthesized but low yields in the final two steps were observed due to the instability of the N^4-acetyl group. Then, a revised protecting group strategy relying on N^4-benzoyl (N^4-Bz) protection was introduced and satisfactory yields were found in the final steps of the amidite synthesis. Thus, we only report the optimized synthetic procedure using N^4-benzoyl protection in the Supplementary Information.

m^5C containing DNA oligonucleotides: The A_6-DNA^{m5C15} single-stranded oligonucleotide was synthesized in-house using a MerMade 6 oligo synthesizer. Standard DNA phosphoramidites (n-ibu-dG, bz-dA, ac-dC, dT, Chemgenes) and a $^{15}N_3$-Ac-m^5dC phosphoramidite were used with a coupling time of 1 min, with the final 5′-DMT group retained during synthesis. The oligonucleotides were cleaved from the supports (1 μmol) using ~ 1 mL of AMA (1:1 ratio of ammonium hydroxide and methylamine) for 30 min and deprotected at room temperature for 2 h. The single strands were then purified using Glen-Pak DNA cartridges and ethanol precipitated.

^{13}C, ^{15}N isotopically labeled DNA oligonucleotides: ^{13}C,^{15}N isotopically labeled DNA single strands were synthesized as described by

Zimmer and Crothers [27], using a chemically synthesized template (from IDT), Klenow fragment DNA polymerase (New England Biolabs) and ^{13}C, ^{15}N isotopically labeled deoxynucleotide triphosphates (Silantes). The reaction mixture was centrifuged to remove excess pyrophosphate, and then subsequently concentrated to 1.5 mL using a 3 kDa molecular weight cutoff centrifugal concentrator (Millipore Sigma). 1.5 mL of a formamide based denaturing loading dye was then added to the reaction mixture, which was then heated at 95 °C for 5 min for denaturation. The mixture was then loaded onto a denaturing gel (20% polyacrylamide/8M urea) for resolution of the target oligonucleotide from other nucleic acid species. Gel bands corresponding to the pure target single strands were identified by UV-shadowing and subject to electroelution (Whatman, GE Healthcare) followed by ethanol precipitation.

^{13}C, ^{15}N isotopically labeled dCTP: Samples of dCTP were prepared by directly dissolving solid ^{13}C, ^{15}N isotopically labeled dCTP in a buffer of the desired pH.

Sample annealing and buffer exchange: Single strands (following ethanol precipitation or as purchased) were re-suspended in water. Duplex samples were prepared by mixing equimolar amounts of the constituent single strands and annealing the sample by heating at T = 95 °C for ~5 min followed by cooling at room temperature for ~1 h. Extinction coefficients for all single and double stranded oligonucleotides were estimated using the ADTBIO oligo calculator (https://www.atdbio.com/tools/oligo-calculator). Extinction coefficients for the modified single strands and duplexes were assumed to be the same as their unmodified counterparts. Modified bases are estimated to affect the extinction coefficient for the oligos used here by <10% based on reference values in Basanta-Sanchez et al. [28]. Following annealing, the samples were exchanged three times into the desired buffer using centrifugal concentrators (4 mL, Millipore Sigma). 10% by volume of D_2O (Millipore Sigma) was added to the samples prior to the NMR measurements.

Buffer preparation: Sodium phosphate buffers for NMR measurements were prepared by the addition of equimolar solutions of sodium phosphate monobasic and dibasic salts, sodium chloride, and EDTA to give final concentrations (unless mentioned otherwise) of 15 mM (phosphate), 25 mM and 0.1 mM respectively. The pH of the buffers was adjusted by the addition of phosphoric acid, after which they were brought up to the desired volume, and filtered and stored for further usage.

2.2. NMR spectroscopy

NMR experiments were performed on a 600 or 700 MHz Bruker Avance 3 spectrometer equipped with triple-resonance HCN cryogenic probes. All experiments were conducted in at pH = 5.4 and at T = 25 °C in NMR buffer unless stated otherwise. The NMR data was processed and analyzed with NMRpipe [29] and SPARKY [30].

Resonance assignments: Amino resonances were assigned using a combination of 2D NOESY and [^{15}N, ^{1}H] HSQC experiments. Assignments for the C6/C1′ resonances were obtained as described previously [5].

Off-resonance $R_{1\rho}$ RD measurements: $R_{1\rho}$ measurements were carried out as described previously for carbon [31] and amino [24] spins, using selective Hartman-Hahn transfers to excite signals corresponding to nuclei of interest. For the amino $R_{1\rho}$ experiment, matched RF fields were applied on the amino nitrogen and the amino proton with the more intense signal in the 2D [^{15}N, ^{1}H] HSQC. Magnetization corresponding to cytosine-N4/cytosine-C6/guanine-C1′ was allowed to relax under an applied spin-lock field for a maximal duration (<120 ms for ^{15}N and < 60 ms for ^{13}C) chosen appropriately to achieve ~70% loss in signal intensity at the end of the relaxation period. The signal intensity was recorded for 4–7 delays equally spaced over the relaxation period. Spin-lock powers used for ^{13}C and ^{15}N $R_{1\rho}$ measurements ranged from 150 to 2200 Hz and 150–600 Hz respectively (Table 5). Absolute offset frequencies were chosen ranging from 0 to 3.5 times the given spin-lock power (Table 5). Offsets greater than 3.5 times the spin-lock power were avoided owing to significant R_1 relaxation contributions [31].

Fitting of $R_{1\rho}$ RD data: $R_{1\rho}$ values for a given spin-lock power offset combination were obtained by fitting the peak intensities as a function of delay time to a mono-exponential function. Bloch-McConnell (B-M) simulations were used to fit $R_{1\rho}$ values as a function of spin-lock power and offset to a two state exchange model [3,25], with the uncertainties in the exchange parameters extracted using a Monte-Carlo scheme as described previously [32].

2.3. Density functional theory calculations

Density Functional Theory (DFT) calculations were performed using Gaussian 09d (Gaussian Inc.) [33] to compute chemical shifts for G-C Watson-Crick and G(*syn*)-C$^+$ Hoogsteen bps, and isolated cytosine nucleosides with and without protonation. The starting structure for the G-C Watson-Crick bp and the cytosine nucleoside were obtained from an idealized G-C bp in B-form DNA, which was constructed using the *fiber* module of the 3DNA suite of programs [34]. The starting structure for the G(*syn*)-C$^+$ Hoogsteen bp and protonated cytosine nucleoside were obtained from the crystal structure (PDB ID: 1QNA) of TATA box binding protein in complex with DNA [10]. For all the calculations, two rounds of geometry optimization were initially performed using the B3LYP functional [35] and the 3-21G [36] and 6-311 + G(2d,p) [37] basis sets, with the positions of all heavy atoms fixed during optimization. NMR chemical shifts were then computed using the GIAO method [38] on the configuration at the end of the second round of optimization. ^{13}C and ^{15}N chemical shifts were referenced to those of carbon and nitrogen in TMS and NH_3 respectively, which were computed at the same level of theory.

3. Results

3.1. Cytosine N4 $R_{1\rho}$ RD provides direct evidence for (G)O6···H_2-N4(C)$^+$ hydrogen bonding in transient G(syn)-C$^+$ Hoogsteen base pairs

Our strategy to detect the (G)O6···H_2-N4(C)$^+$ hydrogen bond in transient G(*syn*)-C$^+$ Hoogsteen bps is to use the cytosine amino nitrogen (N4) as an $R_{1\rho}$ RD probe. The choice of this nucleus is motivated by its direct involvement in the hydrogen bond, the well-known sensitivity of nitrogen chemical shifts to changes in hydrogen bonding [39,40] and the ability to perform $R_{1\rho}$ RD experiments on amino nitrogen atoms. The approach builds on that used in a prior study on G-T mismatches wherein guanine amino N2 $R_{1\rho}$ RD was used to detect the (G)N2-H_2···O2(T) hydrogen bond in transient Watson-Crick like G-T mismatches [24,26]. Although cytosine-N4 is hydrogen bonded in both G-C Watson-Crick and G(*syn*)-C$^+$ Hoogsteen bps, differences in the cytosine-N4 chemical shift can be expected owing to protonation of the base and also possibly due to differences in stacking and hydrogen bonding.

To test whether the cytosine-N4 chemical shift is indeed a sensitive probe of the Watson-Crick to Hoogsteen transition, we first recorded 2D [^{15}N, ^{1}H] HSQC spectra of A_6-DNA and A_6-DNA^{m1G10} duplexes (Fig. 1C) containing Watson-Crick G10-C15 and Hoogsteen m^{1}G10(*syn*)-C15$^+$ bps, respectively (Fig. 2A). In these samples, the DNA strand containing C15 was ^{13}C, ^{15}N isotopically labeled (Fig. 1C). In m^{1}G, the N^1-methyl group biases the conformation of the bp towards Hoogsteen by sterically destabilizing the Watson-Crick conformation and by disrupting a Watson-Crick

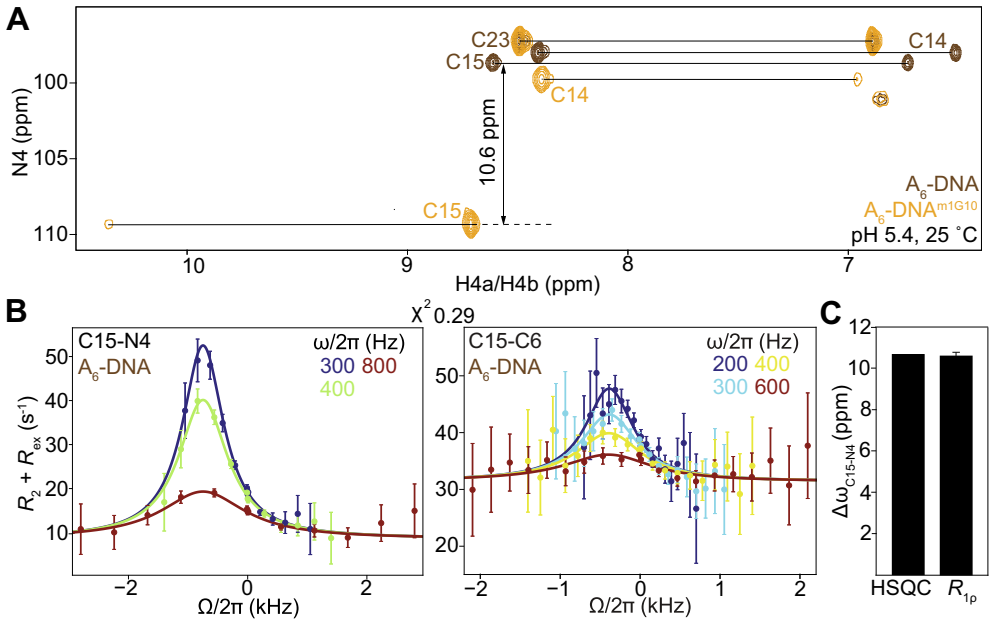

Fig. 2. Using off-resonance cytosine-N4 $R_{1\rho}$ RD to probe a transient G(*syn*)-C$^+$ Hoogsteen bp in duplex DNA. (A) Overlay of 2D [^{15}N, ^{1}H] HSQC spectra of the amino region of A_6-DNA and A_6-DNA^{m1G10}. (B) Off-resonance $R_{1\rho}$ RD profiles for C15-N4 and C15-C6 measured in A_6-DNA. Spin-lock amplitudes are color coded. Solid lines denote shared fits to the RD data using the Bloch-McConnell (B-M) equations assuming a two-state exchange process. The initial alignment of the magnetization during the B-M fitting was performed as described previously [3]. (C) Comparison of the difference in C15-N4 chemical shift ($\Delta\omega_{C15\text{-}N4} = \omega_{C15\text{-}N4}(A_6\text{-}DNA^{m1G10}) - \omega_{C15\text{-}N4}(A_6\text{-}DNA)$) between Hoogsteen m^{1}G(*syn*)-C$^+$ and Watson-Crick G-C bps from 2D HSQC spectra and between Hoogsteen G(*syn*)-C$^+$ and Watson-Crick G-C bps from $R_{1\rho}$ measurements ($\Delta\omega_{C15\text{-}N4} = \omega_{ES} - \omega_{GS}$) (Table 1). Error bars for panels B and C represent the experimental uncertainty obtained while fitting the $R_{1\rho}$ data, as determined by a Monte-Carlo scheme described previously [32]. All measurements were carried out at pH = 5.4 and T = 25 °C in NMR buffer. For the above measurements, the strand containing C15 in A_6-DNA and A_6-DNA^{m1G10} was ^{13}C, ^{15}N isotopically labeled (Fig. 1C).

hydrogen bond (Fig. 1B) [5]. The 2D [^{15}N, ^{1}H] HSQC spectra of A_6-DNA and A_6-DNA^{m1G10} show that that in both the G10-C15 Watson-Crick and m^{1}G10(*syn*)-C15$^+$ Hoogsteen bps, cytosine-N4 is hydrogen bonded, as two separate amino proton signals are observed (Fig. 2A). Overlaying the two spectra, we find that C15-N4 experiences a large downfield shift ($\Delta\omega_{C15\text{-}N4}$ = 10.6 ppm) on formation of a Hoogsteen bp (Fig. 2A). Such sizeable downfield shifts have previously been reported for C(*anti*)-G(*anti*)-C$^+$(*anti*) base triples in which the protonated cytosine forms Hoogsteen hydrogen bonds with the *anti* guanine [41]. These chemical shift perturbations are also in agreement with density functional theory (DFT) calculations [5] carried out on G(*syn*)-C$^+$ Hoogsteen and G-C Watson-Crick bps, which predict $\Delta\omega_{C\text{-}N4}$ = 9.7 ppm (Methods section). The calculations show that this large shift is primarily driven by protonation of cytosine-N3 since even for an isolated cytosine nucleoside, $\Delta\omega_{C\text{-}N4}$ on protonation is calculated to be 13.4 ppm, which is similar to $\Delta\omega_{C\text{-}N4}$ = 10 ppm observed experimentally on protonation of cytosine nucleosides [42]. Nevertheless, we can expect that hydrogen-bonding does contribute to the chemical shift difference of cytosine-N4 between Watson-Crick and Hoogsteen bps as studies employing ^{15}N labeling of the amino groups in the context of nucleic acids have shown that the amino nitrogen chemical shift can vary by 2–4 ppm due to changes in hydrogen bonding alone [43,44], and because the N4 amino chemical shift of a protonated cytosine in a hydrogen bonded m^{1}G-C$^+$ Hoogsteen bp is downfield shifted relative to isolated dCTP$^+$ by ~6.8 ppm (Fig. S1).

Thus, based on the comparison of amino HSQC spectra of A_6-DNA and A_6-DNA^{m1G10}, if transient G(*syn*)-C$^+$ Hoogsteen bps were indeed stabilized by a (G)O6···H$_2$-N4(C)$^+$ hydrogen bond, we would predict cytosine-N4 to experience a ~10.6 ppm downfield change in chemical shift on forming the Hoogsteen bp. In contrast, if the protonated cytosine was not hydrogen bonded in the Hoogsteen bp, a smaller downfield shift of around 6–8 ppm is expected, based on prior studies exploring the sensitivity of the amino nitrogen chemical shift to changes in hydrogen bonding [43,44]. To test the above prediction, we performed off-resonance $R_{1\rho}$ RD measurements on C15-N4 in A_6-DNA at pH = 5.4 and T = 25 °C. As a control, we also measured off-resonance $R_{1\rho}$ RD profiles for C15-C6, which has been shown to be sensitive to cytosine protonation accompanying Hoogsteen bp formation [5,45].

We observed $R_{1\rho}$ RD at C15-C6 as expected for exchange between G-C Watson-Crick and G(*syn*)-C$^+$ Hoogsteen bps [5,45]. The data could be satisfactorily fit to a two-state exchange model involving a dominant ground state (GS) and a sparsely populated excited state (ES) [46] (Fig. S2). The exchange parameters obtained from this fit (p_{ES} = 0.942 ± 0.089%, $k_{ex} = k_1 + k_{-1}$ = 2194 ± 239 s^{-1}, where p_{ES} is the ES population, k_{ex} is the exchange rate and k_1 and k_{-1} are the forward and backward rates, respectively) were in very good agreement with values reported previously for the Watson-Crick to Hoogsteen transition for this G-C bp using other

Table 1
Exchange parameters obtained from two-state fitting of off-resonance $R_{1\rho}$ RD data for C15-N4 and C15-C6 measured in A_6-DNA at pH = 5.4 and T = 25 °C. For these measurements, an A_6-DNA duplex in which the strand containing C15 was ^{13}C, ^{15}N isotopically labeled was used (Fig. 1C).

	C15-N4 (2-state Individual Fit)	C15-C6 (2-state Individual Fit)
p_{ES} (%)	0.720 ± 0.028	0.942 ± 0.089
k_{ex} (s^{-1})	1933 ± 147	2194 ± 239
$\Delta\omega$ (ppm)	10.66 ± 0.18	2.01 ± 0.09
R_1 (s^{-1})	2.48 ± 0.08	2.32 ± 0.09
R_2 (s^{-1})	8.55 ± 0.3	30.35 ± 0.56
	C15-N4 + C15-C6 (2-state Shared Fit)	
p_{ES} (%)	0.740 ± 0.022	
k_{ex} (s^{-1})	1866 ± 106	
$\Delta\omega$ (ppm)	10.58 ± 0.16	2.19 ± 0.07
R_1 (s^{-1})	2.48 ± 0.07	2.20 ± 0.07
R_2 (s^{-1})	8.59 ± 0.25	31.42 ± 0.25

Table 2
Exchange parameters obtained from two-state fitting of off-resonance $R_{1\rho}$ RD data for C15-N4 and G10-C1′ measured in A_6-DNA at pH = 6.8 and T = 25 °C. For these measurements, an A_6-DNA duplex in which both single strands were ^{13}C, ^{15}N isotopically labeled was used (Fig. 1C).

	C15-N4 (2-state Individual Fit)	G10-C1′ (2-state Individual Fit)
p_{ES} (%)	0.035 ± 0.008	0.063 ± 0.016
k_{ex} (s^{-1})	1513 ± 701	1701 ± 899
Δω (ppm)	9.74 ± 1.16	3.25 ± 0.50
R_1 (s^{-1})	4.08 ± 0.02	1.5 ± 0.10
R_2 (s^{-1})	9.01 ± 0.08	14.92 ± 0.19
	C15-N4 + G10-C1′ (2-state Shared Fit)	
p_{ES} (%)	0.039 ± 0.007	
k_{ex} (s^{-1})	1595 ± 611	
Δω (ppm)	9.22 ± 1.04	3.59 ± 0.73
R_1 (s^{-1})	4.09 ± 0.02	1.56 ± 0.08
R_2 (s^{-1})	8.97 ± 0.08	15.13 ± 0.12

base and sugar RD probes (Table 1, Fig. S2) [5,6,22,45]. Indeed, we also observed $R_{1\rho}$ RD for C15-N4 consistent with chemical exchange on the micro-to-millisecond timescale. A two-state fit of the data yield p_{ES} = 0.720 ± 0.028% and k_{ex} = 1933 ± 147 s^{-1} that are in excellent agreement with values obtained for C15-C6 and those reported previously for the Watson-Crick to Hoogsteen transition [5,6,22] (Table 1 and Fig. S2). These results indicate that the ES detected in the C15-N4 RD measurements corresponds to a G(*syn*)-C^+ Hoogsteen bp (Supplementary Discussion). Indeed, the RD data for C15-N4 and C15-C6 could be satisfactorily fit together when sharing the populations and exchange rates (p_{ES} = 0.740 ± 0.022%, k_{ex} = 1866 ± 106 s^{-1}) (Fig. 2B, Table 1).

Fitting of the RD data yielded a sizeable change ($\Delta\omega_{C15\text{-}N4} = \omega_{ES} - \omega_{GS}$ = 10.58 ± 0.16 ppm, where ω_{ES} and ω_{GS} are the chemical shifts of the nucleus in the ES and GS) in the C15-N4 chemical shift between the ES Hoogsteen and GS Watson-Crick bps which is in excellent agreement with the value $\Delta\omega_{C15\text{-}N4}$ = 10.6 ppm predicted based on the difference in C15-N4 chemical shift measured for m^1G(*syn*)-C^+ Hoogsteen bps versus G-C Watson-Crick bps in A_6-DNA (Fig. 2C). This agreement indicates that like the m^1G(*syn*)-C^+ bp, the transient G(*syn*)-C^+ Hoogsteen bp does indeed form a (G)O6···H_2-N4(C)$^+$ hydrogen bond. Similar results were robustly obtained near physiological pH = 6.8 (Fig. S3 and Table 2), which also showed the expected decrease in Hoogsteen bp population relative to pH = 5.4 ($p_{ES,pH\ 5.4}$ = 0.740 ± 0.022%, $p_{ES,pH\ 6.8}$ = 0.039 ± 0.007%). However, because of conformational exchange [45] between m^1G(*syn*)-C^+(*anti*) and m^1G(*anti*)-C(*anti*) geometries of the m^1G-C bp at pH 6.8, where the population of the distorted Watson-Crick m^1G(*anti*)-C(*anti*) bp is nearly 28% , the amino signals are broadened out of detection, preventing comparison of the Δω with that obtained from $R_{1\rho}$, as done at pH 5.4 (Fig. 2C).

3.2. Using cytosine N4 $R_{1\rho}$ RD to measure the Watson-Crick to Hoogsteen exchange at G-m^5C base pairs

As an additional application, we used C-N4 $R_{1\rho}$ RD to examine how methylation of the cytosine at the C5 position impacts the Watson-Crick to Hoogsteen exchange. 5-methylcytosine (m^5C) is one of the most abundant naturally occurring modified bases in DNA that plays important roles in modulating gene expression and regulation [47–49]. Modulation of the dynamics of the

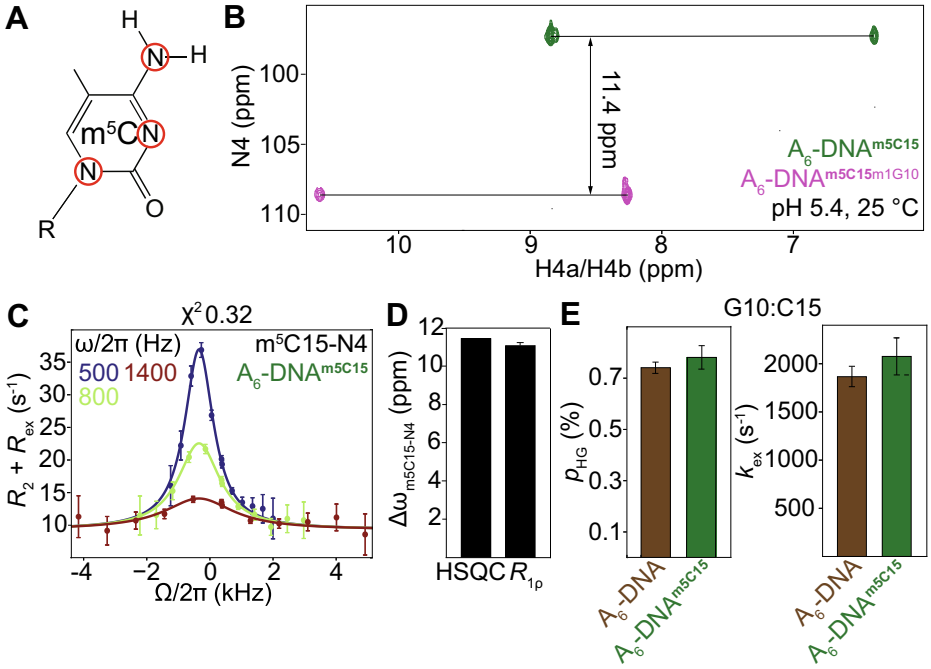

Fig. 3. Using off-resonance cytosine amino $R_{1\rho}$ RD to probe Watson-Crick to Hoogsteen exchange in G-m^5C bps at pH = 5.4 and T = 25 °C in NMR buffer. (A) Chemical structure of m^5C with sites of ^{15}N labeling highlighted with a red circle. (B) Overlay of 2D [^{15}N, ^1H] HSQC spectra of the amino region of A_6-DNA$^{\mathbf{m5C15}}$ and A_6-DNA$^{\mathbf{m5C15}}$m1G10. (C) Off-resonance $R_{1\rho}$ RD profile for m^5C15-N4 in A_6-DNA$^{\mathbf{m5C15}}$. Spin-lock amplitudes are color coded. Solid lines denote a fit of the RD data to the B-M equations assuming a two-state exchange process. The initial alignment of the magnetization during the B-M fitting was performed as described previously [3]. (D) Comparison of the difference in m^5C15-N4 chemical shift ($\Delta\omega_{m5C15\text{-}N4} = \omega_{m5C15\text{-}N4}$($A_6$-DNA$^{\mathbf{m5C15}}$m1G10) − $\omega_{m5C15\text{-}N4}$(A_6-DNA$^{\mathbf{m5C15}}$)) between Hoogsteen m^1G(*syn*)-m^5C^+ and Watson-Crick G-m^5C bps from 2D HSQC spectra, and between Hoogsteen G(*syn*)-m^5C^+ and Watson-Crick G-m^5C bps from $R_{1\rho}$ measurements on A_6-DNA$^{\mathbf{m5C15}}$ ($\Delta\omega_{m5C15\text{-}N4} = \omega_{ES} - \omega_{GS}$) (Table 3). (E) Comparison of the population of the transient Hoogsteen bp (p_{HG}) and the exchange rate (k_{ex}) for the Watson-Crick to Hoogsteen exchange for G10-C15 and G10-m^5C15 bps in A_6-DNA and A_6-DNA$^{\mathbf{m5C15}}$ at pH = 5.4 and T = 25 °C, respectively. Error bars for panels C, D and E represent the experimental uncertainty obtained while fitting the $R_{1\rho}$ data, as determined by a Monte-Carlo scheme described previously [32]. (For interpretation of the references to color in this figure legend, the reader is referred to the web version of this article.)

Table 3
Exchange parameters obtained from two-state fitting of off-resonance $R_{1\rho}$ RD data for m^5C15-N4 measured in A_6-DNA$^{\mathbf{m5C15}}$ at pH = 5.4 and T = 25 °C.

	m^5C15-N4 (2-state Individual Fit)
p_{ES} (%)	0.78 ± 0.046
k_{ex} (s^{-1})	2076 ± 192
Δω (ppm)	11.0 ± 0.16
R_1 (s^{-1})	2.66 ± 0.04
R_2 (s^{-1})	9.33 ± 0.21

Table 4
Exchange parameters obtained from two-state fitting of off-resonance $R_{1\rho}$ RD data for m^5C15-N4 measured in A_6-DNA$^{\mathbf{m5C15}}$ at pH = 6.8 and T = 25 °C.

	m^5C15-N4 (2-state Individual Fit)
p_{ES} (%)	0.037 ± 0.006
k_{ex} (s^{-1})	2323 ± 739
Δω (ppm)	10.13 ± 1.23
R_1 (s^{-1})	1.97 ± 0.03
R_2 (s^{-1})	7.45 ± 0.11

Watson-Crick to Hoogsteen exchange represents a potential avenue by which m^5C could exert its biological effects.

For these studies, we synthesized an m^5C phosphoramidite in which the base moiety was selectively ^{15}N labeled at all ring nitrogen atoms (Fig. 3A and Methods section). We first examined whether m^5C affects hydrogen bonding by comparing 2D [^{15}N, ^1H] HSQC spectra of A_6-DNA containing Watson-Crick G10-m^5C15 (A_6-DNA$^{\mathbf{m5C15}}$) and Hoogsteen m^1G10(*syn*)-m^5C15^+ (A_6-DNA$^{\mathbf{m5C15}\mathrm{m1G10}}$) bps at pH = 5.4 and T = 25 °C (Figs. 1C and 3B).

The observation of two separate amino proton signals indicates that in both Watson-Crick and Hoogsteen conformations, the amino group of m^5C is hydrogen bonded (Fig. 3B). A large downfield shift in the m^5C15-N4 chemical shift ($\Delta\omega_{m5C15\text{-}N4}$ = 11.4 ppm) is observed upon formation of a Hoogsteen bp involving an (m^1G)O6···H_2-N(m^5C)$^+$ hydrogen bond (Fig. 3B). Thus, cytosine N4 $R_{1\rho}$ RD should also be suitable for probing transient G(*syn*)-m^5C^+ Hoogsteen bps.

Next, we used off-resonance cytosine-N4 $R_{1\rho}$ RD to examine how cytosine methylation impacts the Watson-Crick to Hoogsteen exchange. Indeed, we did observe off-resonance $R_{1\rho}$ RD for m^5C15-N4 in A_6-DNA$^{\mathbf{m5C15}}$ at pH = 5.4 and T = 25 °C (Fig. 3C). Fitting the RD data to a two state model yielded $\Delta\omega_{m5C15\text{-}N4}$ = 11.0 ± 0.2 ppm (Table 3), which is again in very good agreement with $\Delta\omega_{C15\text{-}N4}$ = 11.4 ppm obtained from the difference in m^5C15-N4 chemical shift measured for m^1G(*syn*)-m^5C^+ Hoogsteen versus G-m^5C Watson-Crick bps in A_6-DNA (Fig. 3D). This agreement indicates that the transient G(*syn*)-m^5C^+ Hoogsteen bp also forms a (G)O6···H_2-N4(m^5C)$^+$ hydrogen bond.

Importantly, the population (p_{ES} = 0.780 ± 0.046%) and the exchange rate (k_{ex} = 2076 ± 192 s^{-1}) measured for transient G(*syn*)-m^5C^+ Hoogsteen were very similar to values measured for the unmodified G(*syn*)-C^+ Hoogsteen (p_{ES} = 0.740 ± 0.022% and k_{ex} = 1866 ± 106 s^{-1}) (Fig. 3E), indicating that the m^5C modification minimally impacts the thermodynamics or kinetics of Watson-Crick to Hoogsteen exchange. Similar results were obtained when performing experiments at near neutral pH in which the modification minimally impacts the exchange parameters, though as expected the population is reduced for both modified and unmodified samples (Tables 1–4, and Fig. S4).

4. Discussion

One of the most important aspects of nucleic acid structure is the nature of base pairing which is defined by the number and types of hydrogen bonds between nucleotides. The measurement of $R_{1\rho}$ RD data targeting imino nitrogen guanine-N1 and thymine/uracil-N3 [23,50,51] as well as amino nitrogen guanine-N2 [24] has made it possible to probe hydrogen bonding and base pairing in transient low-abundance ESs of DNA and RNA. Here, using RD measurements on cytosine-N4, we have obtained direct evidence in support of the second (G)O6···H_2-N4(C)$^+$ hydrogen bond in transient G(*syn*)-C^+ Hoogsteen bps in canonical duplex DNA. The excellent agreement between the C-N4 chemical shifts in transient G(*syn*)-C^+ and m^1G(*syn*)-C^+ Hoogsteen bps further validates the m^1G mutant as a mimic of the ES G(*syn*)-C^+ Hoogsteen

Table 5
Spin-lock powers ($\omega_1/2\pi$, units Hz) and offsets ($\Omega/2\pi$, units Hz) used in off-resonance $R_{1\rho}$ RD measurements.

	[$\omega_1/2\pi$ (Hz)] [$\Omega/2\pi$ (Hz)]
C15-N4	[300] [−1050, −840, −630, −420, −210, −10, 10, 210, 420, 630, 840, 1050]
A_6-DNA	[400] [−1400, −1120, −840, −560, −280, −10, 10, 280, 560, 840, 1120, 1400]
(pH = 5.4,	[800] [−2800, −2240, −1680, −1120, −560, −10, 10, 560, 1120, 1680, 2240, 2800]
T = 25 °C)	
C15-C6	[200] [−702, −624, −546, −468, −390, −312, −234, −156, −78, −10, 10, 78, 156, 234, 312, 390, 468, 546, 624, 702]
A_6-DNA	[300] [−1053, −936, −819, −702, −585, −468, −351, −234, −117, −10, 10, 117, 234, 351, 468, 585, 702, 819, 936, 1053]
(pH = 5.4,	[400] [−1404, −1248, −1092, −936, −780, −624, −468, −312, −156, −10, 10, 156, 312, 468, 624, 780, 936, 1092, 1248, 1404]
T = 25 °C)	[600] [−2097, −1864, −1631, −1398, −1165, −932, −699, −466, −233, −10, 10, 233, 466, 699, 932, 1165, 1398, 1631, 1864, 2097]
C15-N4	[200] [−702, −585, −468, −351, −234, −117, −10, 10, 117, 234, 351, 468, 585, 702]
A_6-DNA	[300] [−1050, −875, −700, −525, −350, −175, −10, 10, 175, 350, 525, 700, 875, 1050]
(pH = 6.8,	[500] [−1752, −1460, −1168, −876, −584, −292, −10, 10, 292, 584, 876, 1168, 1460, 1752]
T = 25 °C)	[1000] [−3498, −2915, −2332, −1749, −1166, −583, −10, 10, 583, 1166, 1749, 2332, 2915, 3498]
G10-C1′	[150] [−440, −400, −360, −320, −200, −160, −120, 100, 300]
A_6-DNA	[200] [−600, −550, −500, −450, −400, −400, −350, −300, −250, −150, −50, 100, 200]
(pH = 6.8,	[400] [−1150, −1000, −850, −700, −650, −600, −550, −500, −450, −400, −400, −350, −300, −250, −200, −150, −100, 50, 200, 350, 500, 650,
T = 25 °C)	800, 1000]
	[600] [−1800, −1400, −1200, −1000, −800, −700, −600, −550, −500, −450, −400, −400, −350, −300, −250, −200, −100, 200, 400, 600, 1000,
	1400, 1800]
m^5C15-N4	[500] [−1750, −1400, −1050, −700, −350, −10, 10, 350, 700, 1050, 1400, 1750]
A_6-DNA$^{\mathbf{m5C15}}$	[800] [−1750, −1400, −1050, −700, −350, −10, 10, 350, 700, 1050, 1400, 1750]
(pH = 5.4,	[1400] [−4900, −3920, −2940, −1960, −980, −10, 10, 980, 1960, 2940, 3920, 4900]
T = 25 °C)	
m^5C15-N4	[200] [−702, −585, −468, −351, −234, −117, −10, 10, 117, 234, 351, 468, 585, 702]
A_6-DNA$^{\mathbf{m5C15}}$	[300] [−1050, −875, −700, −525, −350, −175, −10, 10, 175, 350, 525, 700, 875, 1050]
(pH = 6.8,	[500] [−1752, −1460, −1168, −876, −584, −292, −10, 10, 292, 584, 876, 1168, 1460, 1752]
T = 25 °C)	[1500] [−5250, −4375, −3500, −2625, −1750, −875, −10, 10, 875, 1750, 2625, 3500, 4375, 5250]

bp. Determining high resolution structure and dynamic ensemble of $m^1G(syn)$-C^+ containing DNA duplexes may provide further insights into the G(*syn*)-C^+ Hoogsteen ES, as recently done for $m^1A(syn)$-T Hoogsteen bps [15,22].

The same strategy used in this work could in principle be applied to examine the (A)N6-H_2···O4(T) hydrogen bond in transient A(*syn*)-T Hoogsteen bps. However, performing $R_{1\rho}$ RD measurements on the adenine amino group is typically hampered by low sensitivity in conventional 2D [^{15}N, ^{1}H] HSQC experiments [52] owing to severe line broadening of ^{1}H signals due to rotation of the amino group on the intermediate chemical shift timescale [53]. This problem could be addressed by using sensitivity enhancement modules [54] or CPMG-INEPT magnetization transfer blocks [55]. Alternatively, one could rely on magnetization transfer to A-N6 from the directly bonded C6 using the relatively large $^1J_{N6\text{-}C6} \sim 20$ Hz [56]. More generally, cytosine amino $R_{1\rho}$ RD experiments could be used to study conformational dynamics in other nucleic acid systems involving changes in hydrogen bonding and base protonation, such as triplexes [57] and i-motifs [58].

The exchange parameters measured for the Watson-Crick to Hoogsteen transition of the G10-C15 bp in A_6-DNA at pH = 5.4, T = 25 °C and 90% H_2O/10% D_2O in this study ($p_{ES} = 0.740 \pm 0.022\%$, $k_{ex} = 1866 \pm 106\ s^{-1}$) differ slightly different from those determined previously [22] using the same buffer conditions but in the presence of 100% D_2O ($p_{ES} = 0.40 \pm 0.01\%$, $k_{ex} = 992 \pm 52\ s^{-1}$). This hints at the presence of both kinetic and thermodynamic isotope effects for the G-C Watson-Crick to G(*syn*)-C^+ Hoogsteen bp exchange; the former could be used to gain insights into the nature of the transition state for formation of a G(*syn*)-C^+ Hoogsteen bp as done in prior studies of the enzyme Ribonuclease A [59], wherein rate-limiting conformational changes gating product release were suggested to involve proton transfer, based on the observation of H/D kinetic isotope effects. Finally, while our studies indicate that for the A_6-DNA sequence context m^5C does not significantly impact the Watson-Crick to Hoogsteen exchange, we cannot rule out larger effects in other sequence contexts, such as CpG dinucleotides in which m^5C is often found [48,49]. Additional studies are required to test this possibility.

Acknowledgements

We thank Laura Ganser for critically reading the manuscript and all members of the Al-Hashimi and Kreutz laboratories for their input. This work was supported by the US National Institutes of Health (R01GM089846) grant to H. M. A, and the Austrian Science Fund FWF (P28725 and P30370) and Austrian Research Promotion Agency FFG (West Austrian BioNMR, 858017) to C. K.

Declaration of Competing Interest

H.M.A. is an advisor to and holds an ownership interest in Nymirum Inc., which is an RNA-based drug discovery company. The research reported in this article was performed by the Duke University faculty and students and was funded by NIH contracts to H.M.A.

Appendix A. Supplementary material

Supplementary data to this article can be found online at https://doi.org/10.1016/j.jmr.2019.106589.

References

[1] D.F. Hansen, P. Vallurupalli, L.E. Kay, Using relaxation dispersion NMR spectroscopy to determine structures of excited, invisible protein states, J. Biomol. NMR 41 (2008) 113–120.
[2] A.G. Palmer 3rd, F. Massi, Characterization of the dynamics of biomacromolecules using rotating-frame spin relaxation NMR spectroscopy, Chem. Rev. 106 (2006) 1700–1719.
[3] A. Rangadurai, E.S. Szymaski, I.J. Kimsey, H. Shi, H.M. Al-Hashimi, Characterizing micro-to-millisecond chemical exchange in nucleic acids using off-resonance R1ρ relaxation dispersion, Progr. Nucl. Magn. Reson. Spectrosc. 112–113 (2019) 55–102.
[4] Y. Xue, D. Kellogg, I.J. Kimsey, B. Sathyamoorthy, Z.W. Stein, M. McBrairty, H.M. Al-Hashimi, Characterizing RNA excited states using NMR relaxation dispersion, Methods Enzymol. 558 (2015) 39–73.
[5] E.N. Nikolova, E. Kim, A.A. Wise, P.J. O'Brien, I. Andricioaei, H.M. Al-Hashimi, Transient Hoogsteen base pairs in canonical duplex DNA, Nature 470 (2011) 498–502.
[6] H.S. Alvey, F.L. Gottardo, E.N. Nikolova, H.M. Al-Hashimi, Widespread transient Hoogsteen base pairs in canonical duplex DNA with variable energetics, Nat. Commun. 5 (2014) 4786.
[7] K. Hoogsteen, The structure of crystals containing a hydrogen-bonded complex of 1-methylthymine and 9-methyladenine, Acta Cryst. 12 (1959) 822–823.
[8] H. Zhou, B.J. Hintze, I.J. Kimsey, B. Sathyamoorthy, S. Yang, J.S. Richardson, H.M. Al-Hashimi, New insights into Hoogsteen base pairs in DNA duplexes from a structure-based survey, Nucl. Acids Res. 43 (2015) 3420–3433.
[9] M. Kitayner, H. Rozenberg, R. Rohs, O. Suad, D. Rabinovich, B. Honig, Z. Shakked, Diversity in DNA recognition by p53 revealed by crystal structures with Hoogsteen base pairs, Nat. Struct. Mol. Biol. 17 (2010) 423–429.
[10] G.A. Patikoglou, J.L. Kim, L. Sun, S.H. Yang, T. Kodadek, S.K. Burley, TATA element recognition by the TATA box-binding protein has been conserved throughout evolution, Genes Dev. 13 (1999) 3217–3230.
[11] J.A. Cuesta-Seijo, G.M. Sheldrick, Structures of complexes between echinomycin and duplex DNA, Acta Crystallogr. D Biol. Crystallogr. 61 (2005) 442–448.
[12] X.L. Gao, D.J. Patel, NMR studies of echinomycin bisintercalation complexes with d(A1-C2-G3-T4) and d(T1-C2-G3-A4) duplexes in aqueous solution: sequence-dependent formation of Hoogsteen A1.T4 and Watson–Crick T1.A4 base pairs flanking the bisintercalation site, Biochemistry 27 (1988) 1744–1751.
[13] H. Yang, Y. Zhan, D. Fenn, L.M. Chi, S.L. Lam, Effect of 1-methyladenine on double-helical DNA structures, FEBS Lett. 582 (2008) 1629–1633.
[14] U.S. Singh, J.G. Moe, G.R. Reddy, J.P. Weisenseel, L.J. Marnett, M.P. Stone, 1H NMR of an oligodeoxynucleotide containing a propanodeoxyguanosine adduct positioned in a (CG)3 frameshift hotspot of Salmonella typhimurium hisD3052: Hoogsteen base-pairing at pH 5.8, Chem. Res. Toxicol. 6 (1993) 825–836.
[15] B. Sathyamoorthy, H. Shi, H. Zhou, Y. Xue, A. Rangadurai, D.K. Merriman, H.M. Al-Hashimi, Insights into Watson-Crick/Hoogsteen breathing dynamics and damage repair from the solution structure and dynamic ensemble of DNA duplexes containing m1A, Nucl. Acids Res. 45 (2017) 5586–5601.
[16] K.A. Bunting, S.M. Roe, A. Headley, T. Brown, R. Savva, L.H. Pearl, Crystal structure of the Escherichia coli dcm very-short-patch DNA repair endonuclease bound to its reaction product-site in a DNA superhelix, Nucl. Acids Res. 31 (2003) 1633–1639.
[17] C.G. Yang, K. Garcia, C. He, Damage detection and base flipping in direct DNA alkylation repair, Chembiochem 10 (2009) 417–423.
[18] D.T. Nair, R.E. Johnson, S. Prakash, L. Prakash, A.K. Aggarwal, Replication by human DNA polymerase-iota occurs by Hoogsteen base-pairing, Nature 430 (2004) 377–380.
[19] R.E. Johnson, L. Prakash, S. Prakash, Biochemical evidence for the requirement of Hoogsteen base pairing for replication by human DNA polymerase iota, Proc. Natl. Acad. Sci. USA 102 (2005) 10466–10471.
[20] E.N. Nikolova, H. Zhou, F.L. Gottardo, H.S. Alvey, I.J. Kimsey, H.M. Al-Hashimi, A historical account of Hoogsteen base-pairs in duplex DNA, Biopolymers 99 (2013) 955–968.
[21] J. Portugal, Do Hoogsteen base pairs occur in DNA?, Trends Biochem Sci. 14 (1989) 127–130.
[22] H. Shi, M.C. Clay, A. Rangadurai, B. Sathyamoorthy, D.A. Case, H.M. Al-Hashimi, Atomic structures of excited state A-T Hoogsteen base pairs in duplex DNA by combining NMR relaxation dispersion, mutagenesis, and chemical shift calculations, J. Biomol. NMR 70 (2018) 229–244.
[23] E.N. Nikolova, F.L. Gottardo, H.M. Al-Hashimi, Probing transient Hoogsteen hydrogen bonds in canonical duplex DNA using NMR relaxation dispersion and single-atom substitution, J. Am. Chem. Soc. 134 (2012) 3667–3670.
[24] E.S. Szymanski, I.J. Kimsey, H.M. Al-Hashimi, Direct NMR evidence that transient tautomeric and anionic states in dG.dT form Watson-Crick-like base pairs, J. Am. Chem. Soc. 139 (2017) 4326–4329.
[25] I.J. Kimsey, E.S. Szymanski, W.J. Zahurancik, A. Shakya, Y. Xue, C.C. Chu, B. Sathyamoorthy, Z. Suo, H.M. Al-Hashimi, Dynamic basis for dG*dT misincorporation via tautomerization and ionization, Nature 554 (2018) 195–201.
[26] I.J. Kimsey, K. Petzold, B. Sathyamoorthy, Z.W. Stein, H.M. Al-Hashimi, Visualizing transient Watson-Crick-like mispairs in DNA and RNA duplexes, Nature 519 (2015) 315–320.
[27] D.P. Zimmer, D.M. Crothers, NMR of enzymatically synthesized uniformly 13C15N-labeled DNA oligonucleotides, Proc. Natl. Acad. Sci. USA 92 (1995) 3091–3095.
[28] M. Basanta-Sanchez, S. Temple, S.A. Ansari, A. D'Amico, P.F. Agris, Attomole quantification and global profile of RNA modifications: Epitranscriptome of human neural stem cells, Nucl. Acids Res. 44 (2016) e26.

[29] F. Delaglio, S. Grzesiek, G.W. Vuister, G. Zhu, J. Pfeifer, A. Bax, NMRPipe: a multidimensional spectral processing system based on UNIX pipes, J. Biomol. NMR 6 (1995) 277–293.
[30] T.D. Goddard, D.G. Kneller, SPARKY 3. San Franscisco: University of California.
[31] A.L. Hansen, E.N. Nikolova, A. Casiano-Negroni, H.M. Al-Hashimi, Extending the range of microsecond-to-millisecond chemical exchange detected in labeled and unlabeled nucleic acids by selective carbon R(1rho) NMR spectroscopy, J. Am. Chem. Soc. 131 (2009) 3818–3819.
[32] J.R. Bothe, Z.W. Stein, H.M. Al-Hashimi, Evaluating the uncertainty in exchange parameters determined from off-resonance R1rho relaxation dispersion for systems in fast exchange, J. Magn. Reson. 244 (2014) 18–29.
[33] M.J. Frisch, G.W. Trucks, H.B. Schlegel, G.E. Scuseria, M.A. Robb, J.R. Cheeseman, G. Scalmani, V. Barone, G.A. Petersson, H. Nakatsuji, X. Li, M. Caricato, A. Marenich, J. Bloino, B.G. Janesko, R. Gomperts, B. Mennucci, H.P. Hratchian, J.V. Ortiz, A.F. Izmaylov, J.L. Sonnenberg, D. Williams-Young, F. Ding, F. Lipparini, F. Egidi, J. Goings, B. Peng, A. Petrone, T. Henderson, D. Ranasinghe, V.G. Zakrzewski, J. Gao, N. Rega, G. Zheng, W. Liang, M. Hada, M. Ehara, K. Toyota, R. Fukuda, J. Hasegawa, M. Ishida, T. Nakajima, Y. Honda, O. Kitao, H. Nakai, T. Vreven, K. Throssell, J.J.A. Montgomery, J.E. Peralta, F. Ogliaro, M. Bearpark, J.J. Heyd, E. Brothers, K.N. Kudin, V.N. Staroverov, T. Keith, R. Kobayashi, J. Normand, K. Raghavachari, A. Rendell, J.C. Burant, S.S. Iyengar, J. Tomasi, M. Cossi, J.M. Millam, M. Klene, C. Adamo, R. Cammi, J.W. Ochterski, R. L. Martin, K. Morokuma, O. Farkas, J.B. Foresman, A.D.J. Fox, Gaussian 09, Revision D.01, Gaussian Inc, Wallingford CT, 2016.
[34] X.J. Lu, W.K. Olson, 3DNA: a software package for the analysis, rebuilding and visualization of three-dimensional nucleic acid structures, Nucl. Acids Res. 31 (2003) 5108–5121.
[35] C. Lee, W. Yang, R.G. Parr, Development of the Colle-Salvetti correlation-energy formula into a functional of the electron density, Phys. Rev. B Condens. Matter 37 (1988) 785–789.
[36] J.S. Binkley, J.A. Pople, W.J. Hehre, Self-consistent molecular orbital methods. 21. Small split-valence basis sets for first-row elements, J. Am. Chem. Soc. 102 (1980) 939–947.
[37] R. Krishnan, J.S. Binkley, R. Seeger, J.A. Pople, Self-consistent molecular orbital methods. XX. A basis set for correlated wave functions, J. Chem. Phys. 72 (1979) 650–654.
[38] K. Wolinski, J.F. Hinton, P. Pulay, Efficient implementation of the gauge-independent atomic orbital method for NMR chemical shift calculations, J. Am. Chem. Soc. 112 (1990) 8251–8260.
[39] B. Goswami, B.L. Gaffney, R.A. Jones, Nitrogen-15-Labeled Oligodeoxynucleotides. 5. Use of 15N NMR To Probe -Bonding in an 06MeG*T Base Pair, J. Am. Chem. Soc. 115 (1993) 3832–3833.
[40] B.L. Gaffney, P. Kung, C. Wang, R.A. Jones, Nitrogen-15-Labeled Oligodeoxynucleotides. 8. Use of 15N NMR To Probe Hoogsteen Hydrogen Bonding at Guanine and Adenine N7 Atoms of a DNA Triplex, J. Am. Chem. Soc. 117 (1995) 12281–12283.
[41] P.L. Nixon, A. Rangan, Y.G. Kim, A. Rich, D.W. Hoffman, M. Hennig, D.P. Giedroc, Solution structure of a luteoviral P1–P2 frameshifting mRNA pseudoknot, J. Mol. Biol. 322 (2002) 621–633.
[42] L.C. Sowers, R. Eritja, F.M. Chen, T. Khwaja, B.E. Kaplan, M.F. Goodman, G.V. Fazakerley, Characterization of the high pH wobble structure of the 2-aminopurine.cytosine mismatch by N-15 NMR spectroscopy, Biochem. Biophys. Res. Commun. 165 (1989) 89–92.
[43] Y. Tanaka, C. Kojima, T. Yamazaki, T.S. Kodama, K. Yasuno, S. Miyashita, A. Ono, A. Ono, M. Kainosho, Y. Kyogoku, Solution structure of an RNA duplex including a C-U base pair, Biochemistry 39 (2000) 7074–7080.
[44] X. Zhang, B.L. Gaffney, R.A. Jones, 15N NMR of a specifically labeled RNA fragment containing intrahelical GU Wobble pairs, J. Am. Chem. Soc. 119 (1997) 6432–6433.
[45] E.N. Nikolova, G.B. Goh, C.L. Brooks 3rd, H.M. Al-Hashimi, Characterizing the protonation state of cytosine in transient G.C Hoogsteen base pairs in duplex DNA, J. Am. Chem. Soc. 135 (2013) 6766–6769.
[46] F.A. Mulder, A. Mittermaier, B. Hon, F.W. Dahlquist, L.E. Kay, Studying excited states of proteins by NMR spectroscopy, Nat. Struct. Biol. 8 (2001) 932–935.
[47] E. Li, C. Beard, R. Jaenisch, Role for DNA methylation in genomic imprinting, Nature 366 (1993) 362–365.
[48] J.A. Law, S.E. Jacobsen, Establishing, maintaining and modifying DNA methylation patterns in plants and animals, Nat. Rev. Genet. 11 (2010) 204–220.
[49] Z.D. Smith, A. Meissner, DNA methylation: roles in mammalian development, Nat. Rev. Genet. 14 (2013) 204–220.
[50] Y. Xue, B. Gracia, D. Herschlag, R. Russell, H.M. Al-Hashimi, Visualizing the formation of an RNA folding intermediate through a fast highly modular secondary structure switch, Nat. Commun. 7 (2016), ncomms11768.
[51] J. Lee, E.A. Dethoff, H.M. Al-Hashimi, Invisible RNA state dynamically couples distant motifs, Proc. Natl. Acad. Sci. USA 111 (2014) 9485–9490.
[52] R. Schnieders, A.C. Wolter, C. Richter, J. Wohnert, H. Schwalbe, B. Furtig, Novel (13) C-detected NMR experiments for the precise detection of RNA structure, Angew. Chem. Int. Ed. Engl. (2019).
[53] R. Michalczyk, I.M. Russu, Rotational dynamics of adenine amino groups in a DNA double helix, Biophys. J. 76 (1999) 2679–2686.
[54] O. Zhang, L.E. Kay, J.P. Olivier, J.D. Forman-Kay, Backbone 1H and 15N resonance assignments of the N-terminal SH3 domain of drk in folded and unfolded states using enhanced-sensitivity pulsed field gradient NMR techniques, J. Biomol. NMR 4 (1994) 845–858.
[55] L. Mueller, P. Legault, A. Pardi, Improved RNA structure determination by detection of NOE contacts to exchange-broadened amino protons, J. Am. Chem. Soc. 117 (1995) 11043–11048.
[56] R. Fiala, V. Sklenar, 13C-detected NMR experiments for measuring chemical shifts and coupling constants in nucleic acid bases, J. Biomol. NMR 39 (2007) 153–163.
[57] M.D. Frank-Kamenetskii, S.M. Mirkin, Triplex DNA structures, Annu. Rev. Biochem. 64 (1995) 65–95.
[58] H.A. Day, P. Pavlou, Z.A. Waller, i-Motif DNA: structure, stability and targeting with ligands, Bioorg. Med. Chem. 22 (2014) 4407–4418.
[59] E.L. Kovrigin, J.P. Loria, Characterization of the transition state of functional enzyme dynamics, J. Am. Chem. Soc. 128 (2006) 7724–7725.